Visual Neuroscience (1992), 9, 181–197. Printed in the USA.

Normalization of cell responses in cat striate cortex

DAVID J. HEEGER

NASA-Ames Research Center, Moffett Field, California and
Department of Psychology, Stanford University, Stanford, California

(Received April 3, 1991; Accepted December 31, 1991)

Abstract

Simple cells in the striate cortex have been depicted as half-wave-rectified linear operators. Complex cells have been depicted as energy mechanisms, constructed from the squared sum of the outputs of quadrature pairs of linear operators. However, the linear/energy model falls short of a complete explanation of striate cell responses. In this paper, a modified version of the linear/energy model is presented in which striate cells mutually inhibit one another, effectively normalizing their responses with respect to stimulus contrast. This paper reviews experimental measurements of striate cell responses, and shows that the new model explains a significantly larger body of physiological data.

Keywords: Striate (primary visual) cortex, Simple cells, Complex cells, Linear operators, Energy mechanisms, Normalization, Divisive suppression, Gain control, Response saturation, Adaptation, Nonspecific suppression

Introduction

A long-standing view of simple cells is that they act like half-wave-rectified linear operators, at least over a limited range of stimulus contrasts (Hubel & Wiesel, 1962; Campbell et al., 1968, 1969). In addition, it is widely believed that complex cells are constructed from linear subunits, and that the subunit outputs are rectified before being combined into the complex cell response. A currently popular model for complex cells is that they act like energy mechanisms that compute the sum of the squared outputs of a quadrature pair of linear subunits (Pollen & Ronner, 1983; Adelson & Bergen, 1985).

The linear/energy model of striate physiology is attractive because the response of a linear/energy mechanism can be completely characterized with a relatively small number of measurements. Unfortunately, the linear/energy model falls short of a complete account of striate physiology.

One major fault with the linear/energy model is the fact that cell responses saturate at high contrasts. The responses of ideal linear operators and energy mechanisms, on the other hand, increase with increased stimulus contrast over the entire range of contrasts.

A second fault with the linear/energy model comes from experiments that reveal nonspecific suppression in cortical cells. Excitation of cortical cells is highly stimulus specific, that is, cells are selective for stimulus orientation, spatial frequency, and direction of motion. This excitatory response to a preferred stimulus can be suppressed by superimposing an additional stimulus. The suppression is largely nonspecific. It is independent of direction of motion, largely independent of orientation, broadly tuned for spatial frequency, and it has broad spatial selectivity.

To explain nonspecific suppression and response saturation, Robson (1988) and Bonds (1989) have suggested that striate cells mutually inhibit one another, effectively normalizing their responses with respect to stimulus contrast.

Normalization of striate cell responses is also motivated from a theoretical point of view. It is commonly believed that information about a visual stimulus, other than its contrast, is represented as the relative responses of collections of cells. For example, the orientation of a grating might be represented as the ratio of the responses of two cells, each with a different orientation tuning. Indeed physiologists have found that the ratio of a cell's responses to two stimuli is largely independent of stimulus contrast (e.g. Albrecht & Hamilton, 1982; see below for more references). But cortical cells, unlike linear or energy mechanisms, have a limited dynamic range: their responses saturate for high contrasts. How is it possible for response ratios to be independent of stimulus contrast, in the face of response saturation? Normalization and automatic gain control are standard engineering techniques for dealing with limited dynamic range. I believe that normalization is fundamental to brain function, not only in primary visual cortex but also in other sensory and nonsensory areas of the brain.

Normalization of striate cells is analogous to retinal light adaptation and gain control (see Sperling & Sondhi 1968, for an example; and Shapley & Enroth-Cugell, 1984, for a review), the purpose of which is to keep the retinal response approximately the same when the level of illumination changes. That way, the brain can proceed to process visual information without having to attend to the light level. The consequence of retinal light adaptation is that much of our perception is invariant with respect to intensity, over a wide range of light levels (for exam-

Reprint requests to: David J. Heeger, Department of Psychology, Building 420, Stanford University, Stanford, California 94305, USA.

ple, the perceived contrast of a grating stimulus is largely invariant with respect to mean intensity). Likewise, the normalization mechanism discussed below allows the brain to process visual information without having to attend further to contrast (for example, the perceived orientation of a grating stimulus is largely invariant with respect to contrast).

This paper attempts to reconcile the linear/energy model with the physiological data. In particular, the linear/energy model is modified by including a divisive normalization nonlinearity. The new model, with divisive normalization, explains a significantly larger body of physiological data. Physiological data on contrast-response curves, contrast adaptation, and nonspecific suppression are reviewed. None of these results are consistent with the linear/energy model, but nearly all of them are consistent with the new model.

Some of the material in this paper has been reported previously (Heeger & Adelson, 1989; Heeger, 1990, 1991). Further results are reported in a companion paper (Heeger, 1992*a*). A similar model was recently proposed by Albrecht and Geisler (1991).

Nomenclature

$I(x,y,t)$	stimulus
$L(t)$	response of linear operator
$f(x,y,t)$	weighting function of linear operator
$h(x,y,t)$	impulse response of linear operator
$A(t), A_i^\phi(t)$	response of half-squared operator
$E(t), E_i(t)$	response of energy mechanism
$\overline{E}_i(t)$	normalized energy
$S_i^\phi(t)$	model simple cell response
$C_i(t)$	model complex cell response
R	response of a model cell, either simple or complex
$B(t)$	time-averaged feedback signal
$V_e(\theta), V_s(\theta)$	orientation-tuning curves
c, c_b, c_m	grating contrast
σ^n	semisaturation constant
ϕ	phase of operator
$R_{\max}$	maximum attainable response
T	threshold
M	maintained discharge
k	constant scale factor

The model

In this section, the building blocks of the model are presented: linear operators, energy mechanisms, half-squaring, and divisive normalization. A nomenclature list is provided to help the reader keep track of mathematical notation. The Results section reviews the experimental data and compares model predictions with experimental results.

This paper treats the visual system as a black box up to the level of striate cortex. No attention is paid to the responses of retinal or geniculate cells. Rather, this paper relates cortical cell responses directly to the time-varying stimulus intensities. In doing so, it is implicitly assumed that the retina is at a fixed state of light adaptation.

Linear operators and energy mechanisms

The response of a linear operator is expressed as a weighted sum, over local space and recently past time, of the stimulus intensities. Mathematically, the response, $L(t)$, of a spatiotemporal linear operator is the inner product in space and the convolution in time of a stimulus, $I(x,y,t)$, with the spatiotemporal weighting function of the operator, $f(x,y,t)$:

$$L(t) = \int\int\int_{-\infty}^{\infty} f(x,y,\tau) I(x,y,\tau - t)\,\mathrm{d}x\,\mathrm{d}y\,\mathrm{d}\tau. \qquad (1)$$

The triple integral in the above equation is simply a weighted sum of the stimulus intensities over space and time. The output response waveform, $L(t)$, is the model equivalent of a poststimulus time histogram (PSTH), a measure of a cell's average response per unit time.

The linear operators considered in this paper have weighting functions with positive and negative subregions. The positive and negative weights are balanced, so the operators give no output for a constant intensity stimulus. Rather, their responses are proportional to stimulus contrast, for stimuli that vary in intensity over space and/or time.

The impulse response, $h(x,y,t)$, of a spatiotemporal linear operator is defined as the "mirror image" of its weighting function, $h(x,y,t) = f(x,y,-t)$. The transfer function of a linear operator is defined as the Fourier transform of its impulse response and it is made up of two parts, the amplitude and the phase responses. A linear operator is completely characterized by either its three-dimensional (3D) spatiotemporal impulse response or its 3D spatiotemporal transfer function.

Two linear operators with the same amplitude response, but with phases that are shifted 90 deg (in space and time), are called a quadrature pair (or Hilbert transform pair). A mechanism that sums the squared outputs of a quadrature pair is called an energy mechanism (Adelson & Bergen, 1985; Pollen & Ronner, 1983). An energy mechanism's response is proportional to the squared contrast of a drifting sine grating stimulus. The response is constant over time, independent of the stimulus phase.

Half-wave-rectification and half-squaring

Cell firing rates are by definition positive, whereas linear operators can have positive or negative outputs. A linear cell with a high maintained firing rate could encode the positive and negative values by responding either more or less than the maintained rate. Striate cells, however, have very little maintained discharge so they cannot truly act as linear operators.

The positive and negative outputs might rather be encoded by two half-wave-rectified operators; one mechanism encoding the positive outputs of the underlying linear operator, the other one encoding the negative outputs. Two such mechanisms are complements of one another, that is, the positive weights of one weighting function are replaced by negative weights in the other. Because of the rectification, only one of the two has a nonzero response at any given time.

In this paper, an alternative form is considered for the rectification: half-squaring. The output of a half-squared linear operator is given by

$$A(t) = \lfloor L(t) \rfloor^2, \qquad (2)$$

where $[x] = \max(x,0)$ is half-wave-rectification, and $L(t)$ is the linear response defined in eqn. (1).

An energy mechanism can be constructed as the average of the outputs of four half-squared linear operators, all four with the same "amplitude response," but with phases in steps of 90 deg. The energy output, $E(t)$, is expressed as

$$E(t) = (1/4)[A^0(t) + A^{90}(t) + A^{180}(t) + A^{270}(t)], \quad (3)$$

where $A^\phi(t)$ is the response of a half-squared linear operator, and where the superscript, ϕ, specifies the operator's phase in degrees.

Divisive normalization

Consider a collection of linear operators and energy mechanisms, with various receptive-field centers (covering the visual field) and with various spatiotemporal frequency tunings. Let $E_i(t)$ be the outputs of each of the energy mechanisms. Normalization, in the model, works by dividing each output by the sum of all of the outputs:

$$\overline{E}_i(t) = \frac{E_i(t)}{\sigma^2 + \sum_i E_i(t)}, \quad (4)$$

where σ^2 is called the semisaturation constant. As long as σ is nonzero, the normalized output will always be a value between 0 and 1, saturating for high contracts.

The underlying linear operators can be chosen so that they tile the frequency domain, i.e. the sum of their squared amplitude responses is the unit constant function (everywhere equal to one). In that case, summing the energy outputs over all spatial positions and all frequencies gives the total Fourier energy of the stimulus. The normalization can also be computed "locally" by summing over a limited region of space and a limited range of frequencies.

The local spatial summation region is left unspecified in this paper for the sake of simplicity. Since the simulations were all done using spatially extended grating stimuli, the spatial pooling of the normalization was unimportant. The local range of frequencies in the summation is discussed further below.

There is a problem with normalization, as it has been presented so far. Eqns. (2–4) express the normalization in a feedforward manner. First, the half-squared outputs are computed, using eqn. (2). Then half-squared outputs are combined to give the energy outputs, using eqn. (3). Finally, the energies are combined to give the normalized energies, using eqn. (4). However, the unnormalized outputs cannot be represented by mechanisms with limited dynamic range (e.g. neurons). The solution is to use a feedback network to do the normalization. Then, the unnormalized outputs need not be explicitly represented as cell output firing rates.

The Appendix gives a simple example demonstrating how normalization can be implemented in a feedback network. One consequence of using a feedback network to achieve the normalization is that the feedback signal must be averaged over time to avoid unstable oscillations in the output. The time constant for averaging the normalization signal is left unspecified in this paper for the sake of simplicity.

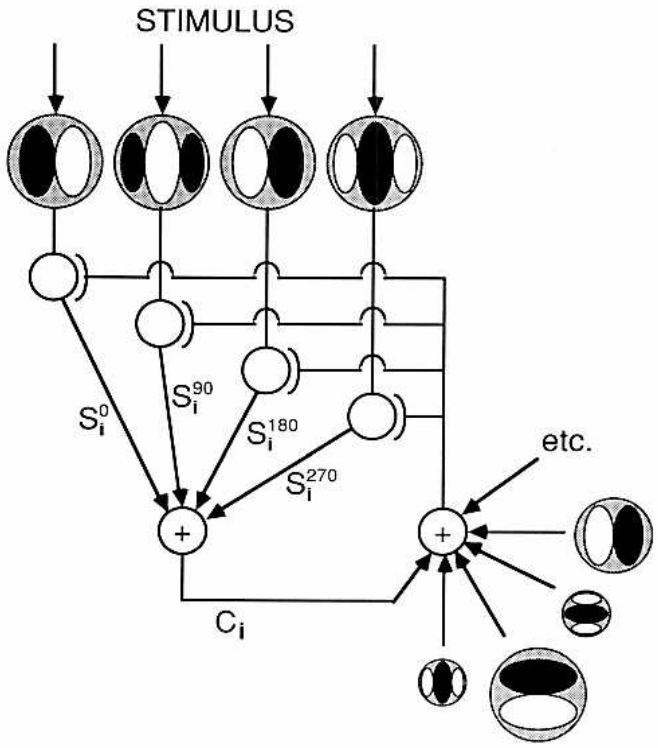

Fig. 1. Diagram of the various stages of the model. Linear weighting functions are depicted as circles, subdivided into excitatory (bright) and inhibitory (dark) subregions. The S_i^ϕ labels represent simple cell outputs, and the C_i label represents a complex cell output. The feedback signal is the combined energy at all orientations and nearby spatial frequencies, averaged over space and time. The feedback signal suppresses the simple cell responses by way of divisive suppression.

Model simple and complex cell responses

The new model in its entirety is depicted in Fig. 1. Simple cells are modeled as normalized, half-squared, linear operators. Complex cells are modeled as normalized energy mechanisms. The normalization signal is combined from all orientations and nearby spatial frequencies.

The various stages of the new model are as follows. Linear operators of four different phases are applied to the stimulus. The outputs of these operators are then half-squared and normalized to give the simple cell responses:

$$S_i^\phi(t) = k \frac{A_i^\phi(t)}{\sigma^2 + \frac{1}{4}\sum_i \sum_\phi A_i^\phi(t)} = k \frac{A_i^\phi(t)}{\sigma^2 + \sum_i E_i(t)}, \quad (5)$$

where S_i^ϕ is the response of a model simple cell with phase ϕ, σ^2 is the semisaturation constant, k is a constant scale factor that determines the maximum attainable firing rate, and $A_i^\phi(t)$ is defined in eqn. (2). The subscript i is used to indicate mechanisms with different spatiotemporal frequency tunings.

The complex cell responses are computed by averaging the simple cell responses:

$$C_i(t) = (1/4)\sum_{\phi} S_i^{\phi}(t),$$

$$= (k/4)\sum_{\phi} \frac{A_i^{\phi}(t)}{\sigma^2 + \frac{1}{4}\sum_i \sum_{\phi} A_i^{\phi}(t)}, \quad (6)$$

$$= k\,\frac{E_i(t)}{\sigma^2 + \sum_i E_i(t)}.$$

Note again that if the underlying linear operators are chosen correctly then the summation in the denominator of eqns. (5) and (6) gives the Fourier energy (squared magnitude of the Fourier transform) of the stimulus within an annulus of spatiotemporal frequencies, over a local region of space and time.

The sections that follow use a particular implementation of the normalization model to compare simulations with physiological data. In this implementation, each filter has a spatial frequency bandwidth of about one octave, and an orientation range of 60 deg. These are arbitrary choices from a theoretical point of view, but they correspond roughly to the average striate cell's tuning widths. The normalization in the present implementation is summed over three spatial frequency bands (another arbitrary choice). The filters tile the frequency domain so the normalization signal is the Fourier energy of the stimulus in a three-octave-wide annulus of spatial frequencies. Operators that differ only in their orientation tuning are all normalized by the same factor. Operators tuned to different spatial frequencies are normalized by different factors, that is, by different three-octave annuli. As mentioned above, the space-time averaging of the normalization signal is left unspecified in this paper for the sake of simplicity.

Results

This section reviews experimental measurements of contrast-response curves, contrast adaptation, and nonspecific suppression. None of these results are predicted by the linear/energy model. This paper shows that nearly all of them can be explained by the new model with divisive normalization.

Throughout this section, model simulation responses are plotted in arbitrary units that are fixed by setting $k = 1$ in eqns. (5) and (6). These units correspond roughly to spikes per second times 0.01. No attempt was made to fit model parameters to the physiological data, so the simulations merely point out the qualitative similarities between the behavior of model cells and real cells. Only one parameter of the model, σ, is varied in the simulations.

Contrast-response

The contrast-response function is a plot of response as a function of contrast, typically measured using sine grating stimuli of optimal spatial frequency and orientation. This section demonstrates that contrast-response of striate cells can be explained by divisive normalization.

Response saturation has commonly been attributed to intracortical suppression (Movshon et al., 1978*a*; Chao-yi & Creutzfeldt, 1984; DeBruyn & Bonds, 1986). DeBruyn and Bonds (1986), for example, used a chemical blocker to remove (GABA mediated) suppression, and found that cells are capable of greater firing rates than those measured under normal conditions. The peak firing rates were more than doubled in some cases.

Saturation of model cells is likewise mediated by intracortical suppression. For model cells, the contrast-response function is sigmoidal (S shaped) when plotted on a log contrast scale. This is qualitatively similar to experimentally measured contrast-response relationships from both cat and primate experiments (Maffei & Fiorentini, 1973; Dean, 1981; Albrecht & Hamilton, 1982; Ohzawa et al., 1982, 1985; Sclar et al., 1990).

The contrast-response functions for visual neurons in lateral geniculate nucleus (LGN) and cortex of both cat and primate have been fitted by the hyperbolic ratio function (Albrecht & Hamilton, 1982; Chao-yi & Creutzfeldt, 1984; Derrington & Lennie, 1984; Sclar et al., 1990):

$$R = R_{\max}\frac{c^n}{\sigma^n + c^n} + M, \quad (7)$$

where R is the evoked response, c is the contrast of the test grating, M is maintained discharge, n is a constant exponent, σ^n is the semisaturation constant, and $R_{\max}$ is the maximum attainable response. With parameters $n = 2$ and $M = 0$, this contrast-response function is equivalent to that of model cells, given by eqns. (5) and (6). The equivalence is easily demonstrated by recalling that the summation, $\sum E_i(t)$, in the denominator of eqns. (5) and (6) is proportional to c^2.

Physiological data from both cat and primate has shown that the exponent in the contrast-response function does not differ significantly between populations of simple and complex cells (Dean, 1981; Albrecht & Hamilton, 1982). The exponent is 2 on average, but there is variability from cell to cell (Albrecht & Hamilton, 1982; Sclar et al., 1990). In the new model, the contrast-response functions of both simple and complex cells have exponents of 2, because of half-squaring.

It is possible to account for some of the variability in contrast-response measurements by adding a threshold parameter to the model. Contrast-response of model cells would then be given by

$$R = R_{\max}\frac{\lfloor c - T \rfloor^n}{\sigma^n + c^n} + M, \quad (8)$$

where T, M, and $n > 0$ are constants. If T is negative and M is positive, then the operator will have a nonzero maintained discharge. If T is positive, then the response of the linear operator must be greater than the threshold, T, to contribute to the output. Half-squaring corresponds to the case in which $n = 2$ and $T = 0$. Half-wave rectification corresponds to the case in which $n = 1$ and $T = 0$. Over-rectification corresponds to the case in which $n = 1$ and $T > 0$.

Varying T in eqn. (8) not only changes the threshold level, but also changes the shape of the contrast-response curve. Varying T and σ simultaneously can look very much like a change in the exponent n. This suggests the possibility of fitting contrast-response data with a fixed exponent, accounting for the variability from cell to cell by changing the values of T and σ.

Contrast gain control

Numerous studies have shown that nearly all neurons in the cat's striate cortex adapt to prolonged stimulation (Maffei et al.,

1973; Vautin & Berkeley, 1977; von der Heydt et al., 1978; Movshon & Lennie, 1979; Ohzawa et al., 1982, 1985; Dean, 1983; Albrecht et al., 1984; Hammond et al., 1985, 1986, 1988, 1989; Marlin et al., 1988; Maddess et al., 1988; Saul & Cynader, 1989*a*, *b*; Bonds, 1991). There is general consensus that geniculate cells do not exhibit adaptation (Movshon & lennie, 1979; Ohzawa et al., 1985; Bonds, 1991). Thus, adaptation must be due to intracortical interactions.

Ohzawa et al. (1982, 1985) adapted cells using drifting gratings of various contrasts. For each adapting contrast (each adaptation state), they measured contrast-response curves. Their data, replotted in Fig. 2A, shows that different adapting contrasts resulted in different contrast-response curves. The contrast-response functions shift from one to the next along the log contrast axis. Similar results have been reported by others (Dean, 1983; Albrecht et al., 1984; DeBruyn & Bonds, 1986; Saul & Cynader, 1989*a*).

Dean (1983) reported a "change of slope" of the contrast-response curve, when plotted on linear axes. This "change of slope" is somewhat difficult to interpret because the contrast-response function is not a line, and thus does not have a single slope for all stimulus contrasts. If it were a line, then the change of slope on linear axes could be interpreted as a downward shift and/or a rightward shift on log-log axes. Thus, characterizing the effect as a "change of slope" is not nearly as informative.

Changing σ in the model leads to a similar shift of the contrast-response relationship, as shown in Fig. 2B. The value of σ specifies a model cell's adaptation level (or gain). Mathematically, consider replacing σ in eqn. (7) with some other value, $k\sigma$. Then the response becomes

$$R(c,\sigma) = R_{\max}\frac{c^n}{(k\sigma)^n + c^n} + M,$$

$$= R_{\max}\frac{(c/k)^n}{\sigma^n + (c/k)^n} + M. \qquad (9)$$

Scaling σ by a constant factor k is the same as scaling the contrast by $1/k$.

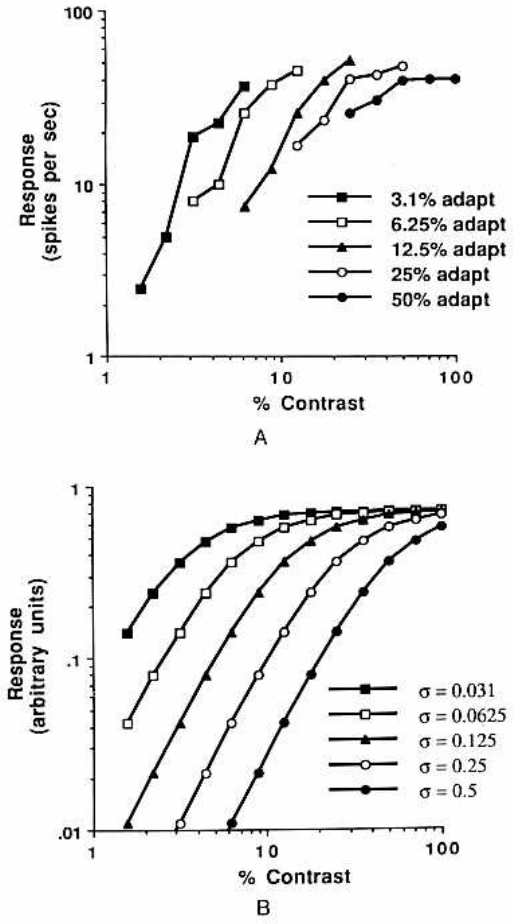

Fig. 2. Effect of adaptation on contrast-response. A: Contrast-response function for a complex cell, replotted from Ohzawa et al. (1985). Stimuli were drifting gratings of optimal spatiotemporal frequency. Each curve is for an adapting stimulus with a different contrast. B: Contrast-response for a model complex cell, for sine grating stimuli of optimal spatial frequency and orientation. Each curve is for a different value of σ. The curves shift laterally on the log-log plots as adapting state changes.

Mechanism for adaptation

What is the mechanism for adaptation that controls the value of σ? Two alternative mechanisms have been proposed. The first possibility is that σ is calibrated independently by each cell, based on that individual cell's response history. A "self-recalibration" mechanism of this sort was proposed by Ullman and Schechtman (1982). The second possibility is that a cell's gain is derived from the pooled responses of a number of cells.

This second possibility is much the same as divisive normalization. There are two differences between the normalization and the gain control. First, gain control is relatively slower than normalization, so σ is averaged with a much longer time constant. Second, σ cannot be allowed to vary without bound. If σ is zero then the quotients in eqns. (5) and (6) will blow up at low contrasts, resulting in infinite responses.

There is evidence (reviewed in the following paragraphs) indicating that both mechanisms are involved in gain control of striate cells. Bonds (1991) suggests that the first mechanism (self recalibration) is dominant when cells are exposed for long time periods to high-contrast stimuli, and that the second mechanism (gain control based on pooled responses) is dominant for shorter exposures to low-contrast stimuli. In either case, σ cannot be allowed to vary without bound. If σ is zero, then the quotients in eqns. (5) and (6) will blow up at low contrasts, resulting in infinite responses.

Consistent with the self-recalibration mechanism, experimenters have found that adaptation is more pronounced when the adapting stimulus evokes a big response (Maffei et al., 1973; Vautin & Berkeley, 1977; Ohzawa et al., 1985; Maddess et al., 1988; Hammond et al., 1988, 1989; Saul & Cynader, 1989*a*, *b*).

Consistent with the second mechanism (gain control based on pooled responses), researchers (Maffei et al., 1973; Saul & Cynader, 1989*a*; Nelson et al., 1991) measured aftereffects when the adapting stimulus was presented only outside the classical receptive field. In addition, Ohzawa et al. (1985) reported anecdotally that many cells appeared to be adapted by stimuli of nonoptimal orientation or spatial frequency. In all of these cases, the adapting stimulus evoked little or no response, but did result in adaptation.

Bonds (1991) has recently confirmed the anecdotal report by Ohzawa et al. (1985). Bonds measured responses to drifting grating stimuli while varying contrast. In every cell studied, response to a given contrast level was lower when that level was preceded by a higher contrast than when it was preceded by a

lower contrast. The effect seemed to have no lower limit; contrasts as low as 3% were effective in response reduction. The effect depended on stimulus contrast and not on response amplitude; the effect was just as big when the cell was adapted by stimuli of nonoptimal orientation.

Further evidence for the second mechanism (gain control based on pooled responses) is provided from studies that used chemicals to modify cell firing rates. Vidyasagar (1990) found that adaptation was not affected when a cell's firing rate was reduced by application of GABA; spike activity was unnecessary for adaptation to occur. In addition, DeBruyn and Bonds (1986) and Vidyasagar (1990) found that adaptation was unaffected when a cell's firing rate was increased by application of bicuculline, a GABA antagonist.

Unexplained adaptation results

There are, however, some adaptation results that cannot be explained simply by changing a cell's gain (σ value). First, Albrecht et al. (1984) found some amount of downward shift of the contrast–response curves in addition to the rightward shift. This is not explained by changing σ in the model.

A second result that is inconsistent with the model is that adaptation changes a cell's spatiotemporal frequency tuning. After long exposure to a high-contrast grating, the response to that grating is often reduced more than its response to other gratings (Movshon & Lennie, 1979; Albrecht et al., 1984; Saul & Cynader, 1989*a*,*b*).

A third unexplained result is that adaptation changes a cell's motion selectivity (this is perhaps the physiological substrate for motion aftereffects). Saul and Cynader (1989*b*) adapted cells with gratings drifting in one direction and tested with gratings drifting in both directions. They confirmed previous reports (von der Heydt et al., 1978; Hammond et al., 1985, 1986, 1988; Marlin et al., 1988) that the adapted direction is affected more than the opposite direction.

These unexplained adaptation phenomena generally occur only after long-term exposure to high-contrast stimuli. Bonds (1991), therefore, argues that these phenomena are due to the second (self-recalibration) adaptation mechanism, and that this mechanism does *not* have a significant impact under normal, day-to-day viewing conditions.

Relative responses are independent of contrast

Consider the response of a linear operator when presented with two different stimuli. If both stimuli are multiplied by the same factor, then the ratio of the responses to the two stimuli remains unchanged. Without normalization, the responses of linear and energy mechanisms increase with stimulus contrast over the entire range of contrasts. With normalization, model cells saturate at high contrasts. In this section, it is demonstrated that (in spite of saturation) the response ratio to two different stimuli is still largely independent of stimulus contrast. This is true both for model cells and for real cells.

Contrast–response for nonoptimal stimuli

The contrast–response curve of a model cell shifts downward (on log–log axes) if the orientation of a test grating is nonoptimal. To demonstrate this fact, the model cell's response is expressed in terms of the grating contrast and orientation. Let $V_e(\theta)$ be the orientation-tuning curve of underlying linear operator. From eqns. (5–7), the model cell's response is given by

$$R(c,\theta) = R_{\max} \frac{c^2 V_e^2(\theta)}{\sigma^2 + c^2}. \tag{10}$$

The value of the numerator depends on stimulus orientation because the underlying linear operator is orientation tuned. However, the value of the denominator does not depend on stimulus orientation because the suppression is pooled over all orientations. The ratio of responses for two different stimulus orientations is given by

$$\frac{R(c,\theta_1)}{R(c,\theta_2)} = \frac{V_e^2(\theta_1)}{V_e^2(\theta_2)}, \tag{11}$$

that is independent of contrast.

If the suppression was broadly tuned for orientation, then the contrast–response curves would shift downward and rightward. The relative amount of rightward shift would depend on the breadth of the tuning. Let $V_e(\theta)$ be the orientation-tuning curve of underlying linear operator, and $V_s(\theta)$ be the orientation-tuning curve of the suppression. The response of a model cell is now given by

$$\begin{aligned} R(c,\theta) &= R_{\max} \frac{c^2 V_e^2(\theta)}{\sigma^2 + c^2 V_s^2(\theta)}, \\ &= R_{\max} \frac{V_e^2(\theta)}{V_s^2(\theta)} \frac{c^2}{(\sigma/V_s)^2 + c^2}. \end{aligned} \tag{12}$$

Varying the stimulus orientation away from optimal causes two things to happen. The value of $(V_e/V_s)^2$ decreases resulting in downward shift, and the value of $(\sigma/V_s)^2$ increases resulting in the rightward shift.

Downward shifts of contrast–response have been measured physiologically by Chao-yi and Creutzfeldt (1984) for stimuli of nonoptimal orientation, for stimuli of nonpreferred direction of motion, and for stimuli in the nondominant eye. Chao-yi and Creutzfeldt, and other authors, interpreted these results as demonstrating that saturation of the contrast–response curve is already present at the precortical level and therefore not due to intracortical mechanisms. On the contrary, the model exhibits the downward shift precisely because of mutual suppression between cortical cells.

Albrecht and Hamilton (1982) recorded similar downward shifts of contrast–response curves for stimuli of nonoptimal spatial frequency, and they also found a slight rightward shift of the curves. Their data is replotted in Fig. 3A. Fig. 3B shows the contrast–response curves of a model cell for various stimulus spatial frequencies. The curves shift mostly downward and slightly rightward for nonoptimal spatial frequencies. The small rightward shift occurs because the suppression is broadly tuned for spatial frequency. If the suppression were equal for all spatial frequencies, then there would be no rightward shift.

Researchers have reported that the "slopes" of contrast–response curves are lowered when using stimuli of nonoptimal orientation (Sclar & Freeman, 1982), nonoptimal direction of movement (Dean, 1980), and nonoptimal spatial or temporal frequency (Dean, 1981; Holub & Morton-Gibson, 1981). As mentioned above ("Contrast gain control"), this "change of slope" is somewhat difficult to interpret because the contrast–response function is not a line, and thus does not have a single slope for all stimulus contrasts. If it were a line, then the change

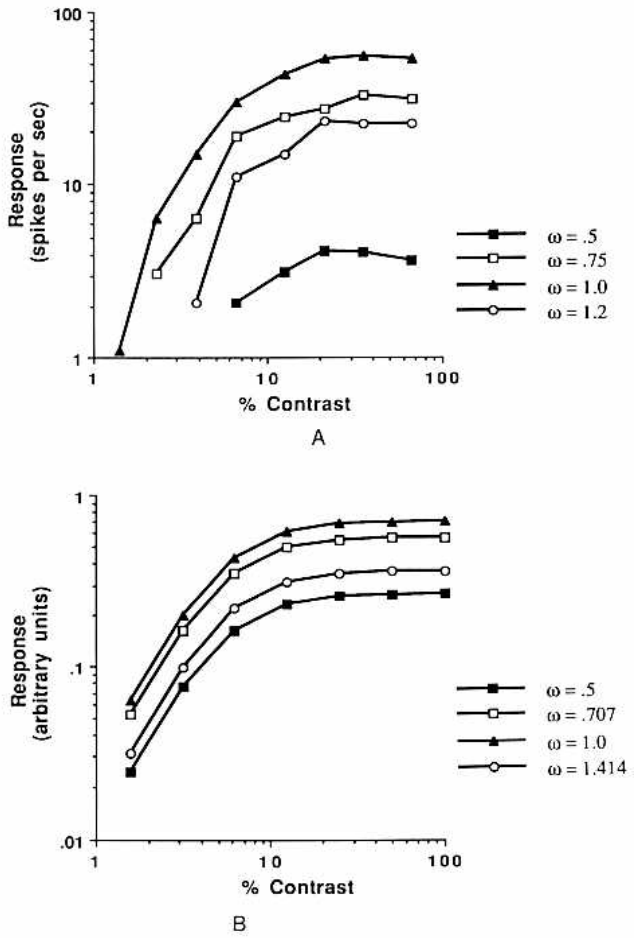

Fig. 3. Response *vs.* contrast as the spatial frequency, ω, of the stimulus is varied. A: Data replotted from Albrecht and Hamilton (1982). B: For a model complex cell, the contrast-response curve shifts downward and very slightly rightward (not visible in the graph) in the log–log plot if the spatial frequency of the test grating is nonoptimal.

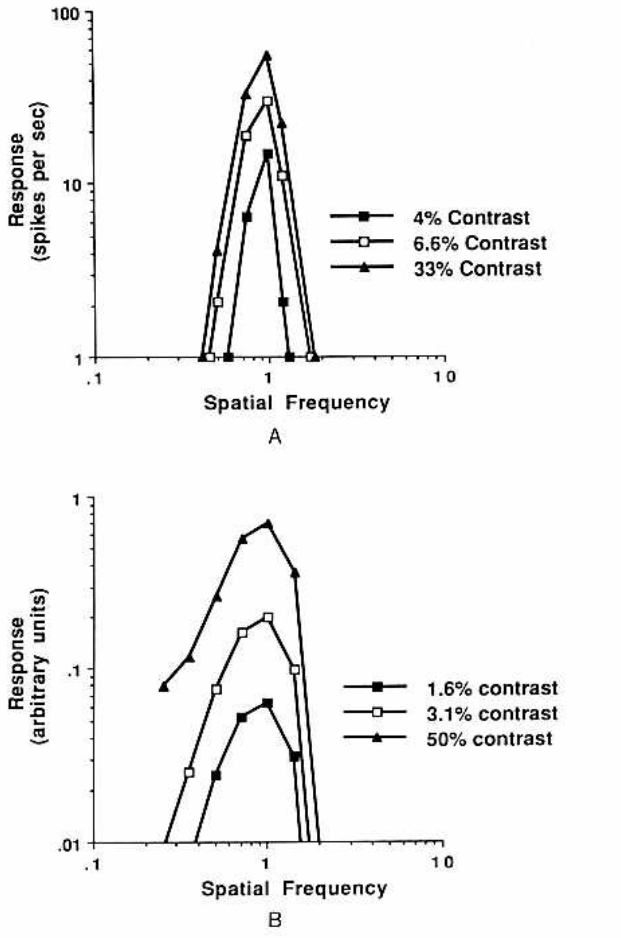

Fig. 4. Spatial-frequency tuning curves as the contrast of the stimulus is varied (same data as in the previous figure plotted in a different way). A: Data replotted from Albrecht and Hamilton (1982). B: For a model complex cell, the tuning width is largely invariant with respect to contrast. Width broadens very slightly (not visible in the graph) with increased contrast.

of slope on linear axes could be interpreted as a downward shift and/or a rightward shift on log–log axes. Thus, characterizing the effect as a "change of slope" is not nearly as informative.

Tuning widths are independent of contrast

The orientation-tuning width of model cells is invariant with respect to contrast. As demonstrated above, the ratio of responses for two different stimulus orientations is independent of contrast. Contrast has no impact on tuning width because the suppression is pooled equally over all stimulus orientations. If the suppression was broadly tuned for orientation, then the model cell's tuning width would depend slightly on contrast.

Physiologists have indeed found that orientation and spatial-frequency tuning widths are roughly constant as contrast is varied (Sclar & Freeman, 1982; Albrecht & Hamilton, 1982; Chao-yi & Creutzfeldt, 1984; Skottun et al., 1987). Experimental results from Albrecht and Hamilton (1982) are replotted in Fig. 4A, and model simulation results are shown in Fig. 4B. Note that Figs. 3 and 4 show the same data plotted in different ways. The spatial-frequency bandwidth of model cells broadens (but only very slightly) with increased contrast, because the suppression is broadly tuned for spatial frequency.

Nonspecific suppression

A number of physiologists have reported that the excitatory response to a preferred stimulus can be suppressed by superimposing an additional stimulus. This suppression has been found to be largely nonspecific. It is independent of direction of motion, largely independent of orientation, broadly tuned for spatial frequency, and it has broad spatial selectivity (Blakemore & Tobin, 1972; Bishop et al., 1973; Maffei & Fiorentini, 1976; Nelson & Frost, 1978; Hammond & MacKay, 1978, 1981; Dean, 1980; Sclar & Freeman, 1982; Morrone et al., 1982; DeValois & Tootell, 1983; Chao-yi & Creutzfeldt, 1984; DeValois et al., 1985; Kaji & Kawabata, 1985; Gulyas et al., 1987; Bonds, 1989; Bonds et al., 1990; Robson et al., 1991; Nelson, 1991; DeAngelis et al., 1992). Some of these researchers have also found that the suppression is interocular, but Ferster (1981), Ohzawa and Freeman (1986), Freeman et al. (1987), and DeAngelis et al. (1992) found this not to be the case.

In the remainder of this section, the results obtained by Bonds (1989) are considered because they are the most recent and the most quantitative. It is shown that nonspecific suppression is divisive and that it can be explained by normalization.

Responses to pairs of gratings, varying orientation

Bonds (1989) measured responses to pairs of sine gratings, a base grating of optimal orientation superimposed on a mask grating of variable orientation. He found that a cell's response may be suppressed for certain mask orientations (cross-orientation suppression). Data from one cell is replotted in Figs. 5A and 5B. Fig. 5A shows the cell's orientation-tuning curve, its response to a single grating as a function of orientation. Fig. 5B shows what happens when the second (mask) grating is superimposed. The horizontal dotted line is the response to the optimally oriented base grating. The solid curve is the response when a second grating of variable orientation was superimposed upon the first. The response of the cell was suppressed at nearly all mask orientations. Model cells exhibit similar behavior, as shown in Figs. 5C and 5D, due to divisive normalization.

Results from another cell, and from another simulation, are shown in Figs. 6A and 6B, respectively. In this figure, the responses were enhanced for some mask orientations near the cell's preferred orientation, and they were suppressed at other mask orientations.

For Figs. 5 and 6, all of the parameters of the model were held fixed except for the value of σ. The simulation result in Fig. 5D was computed with a small value for σ. When the mask grating was optimally oriented, the response increased only slightly above the dotted line. Superimposing the mask grating did not increase the response by much because the response was already nearly saturated. The simulation result in Fig. 6B was computed with a larger value for σ. The response was enhanced for mask orientations near the optimum orientation (the cell was not already saturated), and it was suppressed for nonoptimal mask orientations.

The width of the simulated orientation-tuning curve (Fig. 5C) is precisely the same as the widths of the simulated cross-orientation suppression curves (Figs. 5D and 6B), because there is an equal amount of suppression from all mask orientations [the denominators in eqns. (5) and (6) depend only on contrast, not on orientation].

For real cells, the orientation-tuning and cross-orientation suppression curves are also similar (e.g. compare Figs. 5A and 5B). Some physiological data, however indicate that there is more suppression for mask gratings at the cell's preferred orientation, i.e. that the suppression is broadly tuned for orientation (Bonds, 1989). Cross-correlation experiments by Hata et al. (1988) also argue for broadly tuned suppression. They found mutual intracortical suppression between striate cells only with similar orientation preferences, separated by less than 45 deg.

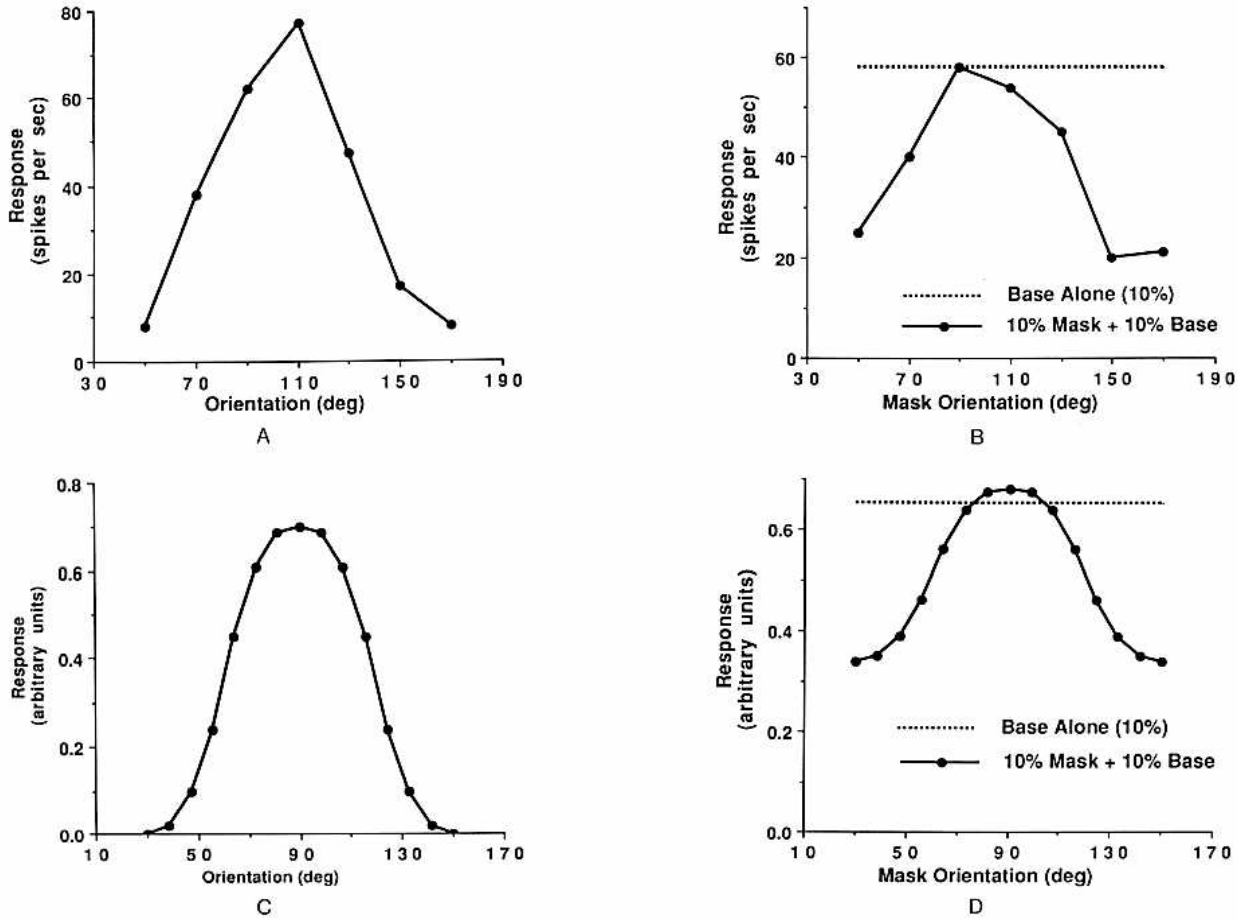

Fig. 5. A: Orientation tuning of a complex cell, replotted from Bonds (1989). B: Cross-orientation suppression measured from the same cell, replotted from Bonds (1989). Horizontal dotted line is response to a single 10% contrast base grating of the cell's preferred orientation. Solid curve is response to 10% contrast base plus 10% contrast mask as a function of the orientation of the mask grating. Base and mask gratings share the same spatial frequency. C: Orientation tuning of a model complex cell. D: Cross-orientation suppression for a model complex cell with $\sigma = 0.03$.

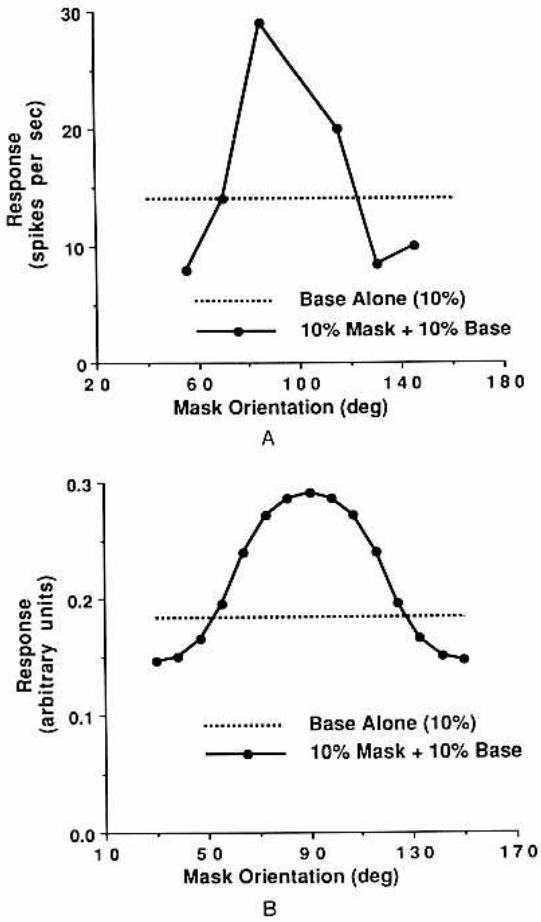

Fig. 6. A: Cross-orientation suppression measured from a complex cell, replotted from Bonds (1989). B: Cross-orientation suppression for a model complex cell with $\sigma = 0.17$.

By contrast, the operators in the model are separated by 60 deg in orientation tuning. The model could certainly be amended to account for these results by using broadly tuned suppression.

On the other hand, DeAngelis et al. (1992) found that *all* cells can be substantially suppressed by an orthogonal grating (so long as the orthogonal grating is restricted to the excitatory region of the receptive field, the spatial frequency of the orthogonal grating is appropriate, and its contrast is sufficiently high).

Some researchers have argued that broadly tuned suppression should serve to sharpen a cell's orientation-tuning curve. In the section "Relative responses are independent of contrast," however, it is shown that broadly tuned suppression behaves only slightly differently from suppression that is not at all orientation selective. The same is true for suppression that is broadly tuned for orientation, for spatial frequency, or for spatial position. The normalization works properly as long as the suppression is sufficiently broad compared to the excitatory tuning of the underlying linear operators.

Responses to pairs of gratings, varying frequency

Bonds (1989) has also reported suppression from nonoptimal spatial frequencies (cross-frequency suppression). Fig. 7B shows the results of an experiment in which the orientation of the mask grating was fixed while its spatial frequency was varied. The horizontal dotted line shows the response to a base grating with optimal spatial frequency. The solid curve is the response when a second grating of variable spatial frequency was superimposed upon the base grating. The mask grating orientation was chosen at the limit of the cell's orientation-tuning curve, so that it did not enhance response for any mask spatial frequency. Suppression from the mask grating is broadly tuned for spatial frequency, as compared with the excitatory spatial-frequency tuning curve for the same cell shown in Fig. 7A. Model cells exhibit similar behavior, as shown in Figs. 7C and 7D.

Although the results are similar, there are some notable differences between the real and simulated data in Fig. 7. The model cell's suppression is more broadly tuned for spatial frequency, especially at the lower contrast. The breadth of the suppression is not a critical aspect of the model, so long as it is sufficiently broad compared to the excitatory tuning of the underlying linear operators (see section "Relative responses are independent of contrast"). However, the model predicts that the breadth of the suppression not depend on contrast. For the real cell, the suppression appears broader at the higher mask contrast.

Responses to pairs of gratings, varying contrast

The data in Fig. 7B demonstrates that the suppression is contrast dependent, since a mask grating of higher contrast results in greater suppression. Several physiologists (Dean et al., 1980; Morrone et al., 1982; Bonds, 1989) measured the magnitude of the suppression as a function on contrast. Figs. 8A and 8B show the responses of a real cell (data replotted from Bonds, 1989) and a model cell for a variety of base and mask contrasts. Each curve is the response for a fixed mask contrast, as the base contrast was varied. Increasing the mask contrast leads to a lateral shift of the contrast–response curves, for both model cells and real cells.

Mathematically, the response of a model cell may be expressed as a function of the contrasts of the base and mask gratings:

$$R(c_b, c_m) = R_{\max} \frac{c_b^n}{\sigma^n + c_b^n + c_m^n}, \qquad = R_{\max} \frac{c_b^n}{(\sigma^n + c_m^n) + c_b^n}, \tag{13}$$

where c_b is the base contrast and c_m is the contrast of a mask grating oriented at the limit of the cell's orientation tuning curve. Changing the mask contrast has the same effect as changing the value of σ. We know (section "Contrast gain control") that changing σ results in lateral shift.

These results indicate that nonspecific suppression is *divisive*. Changing the mask contrast has the same effect as changing the cell's gain.

Surround suppression

A number of researchers have observed that the receptive fields of most striate cells are surrounded by suppressive regions (Blakemore & Tobin, 1972; Bishop et al., 1973; Hess et al., 1975; Maffei & Fiorentini, 1976; Nelson & Frost, 1978; Hammond & MacKay, 1978, 1981; DeValois et al., 1985; Gilbert & Weisel, 1990; Bonds et al., 1990; DeAngelis et al., 1990). The surrounding region is not considered part of the classical receptive field because stimulation in the region does not, by itself,

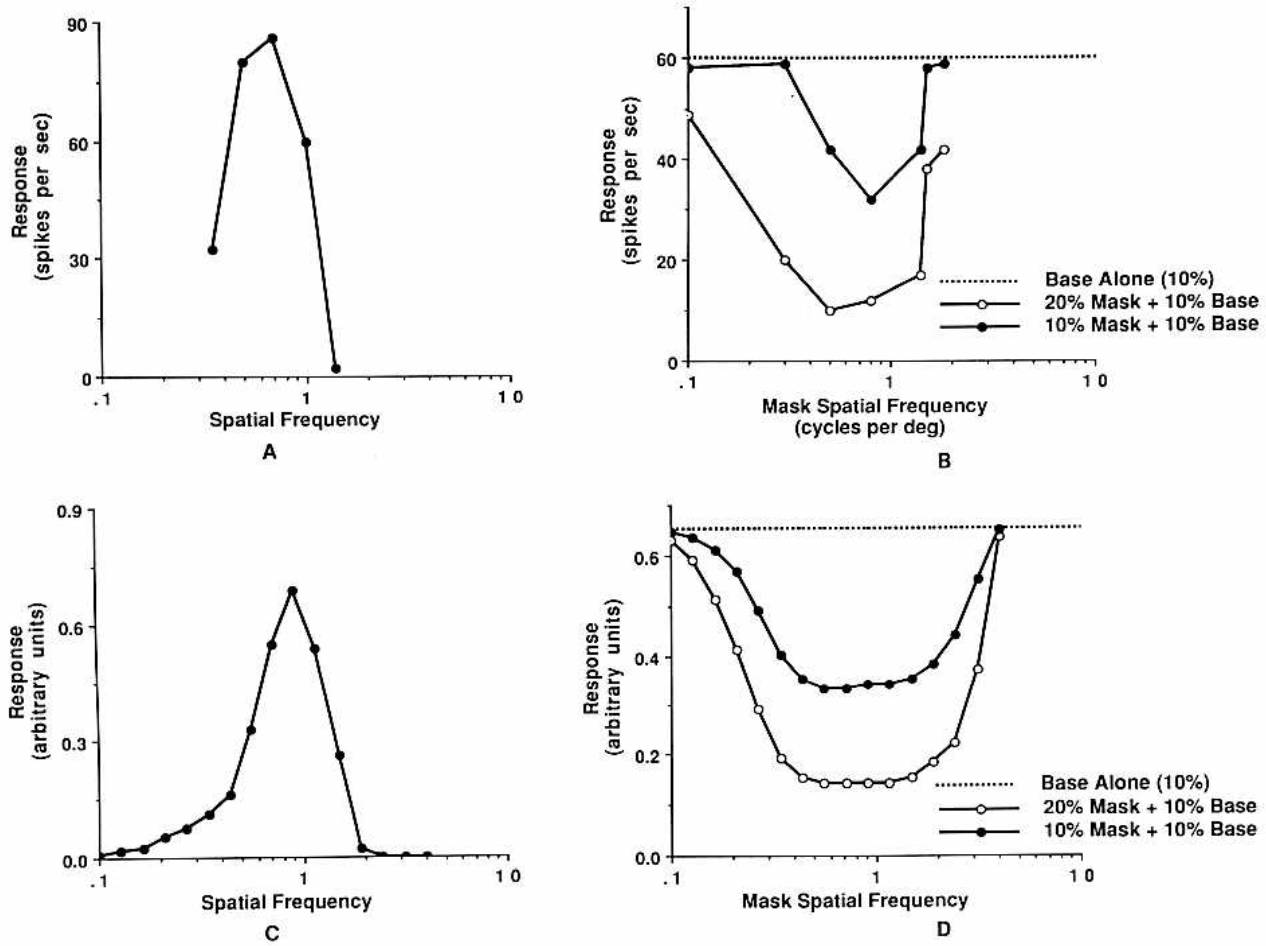

Fig. 7. A: Spatial-frequency tuning of a complex cell, replotted from Bonds (1989). B: Cross-frequency suppression measured from the same cell, replotted from Bonds (1989). Horizontal dotted line is response to a single 10% contrast base grating of the cell's preferred spatial frequency. Solid curve is response to 10% contrast base plus mask as a function of the spatial frequency of the mask grating. Mask contrast was either 10% (closed circles) or 20% contrast (open circles). Base grating was optimally oriented and mask grating oriented at the limit of the cell's orientation tuning curve. C: Spatial-frequency tuning of a model complex cell. D: Cross-frequency suppression from the model cell with $\sigma = 0.03$. Mask grating oriented 60 deg from optimum near the limit of the orientation-tuning curve.

evoke a response. Even so, stimulation in the region outside of the classical receptive field suppresses responses to stimuli placed within the classical receptive field.

In this paper, the spatial pooling of the normalization signal has been left unspecified. Since the simulations were all done using spatially extended grating stimuli, the spatial organization of the normalization was unimportant. Surround suppression could be explained by a "center-surround" spatial organization, in which the normalization signal is averaged over a large spatial area (large compared to the size of the underlying linear operators).

Consistent with divisive normalization, Maffei and Fiorentini (1976) found that the surround did *not* serve to sharpen the cell's orientation tuning. Rather, stimulation in the surround resulted in a downward shift of the tuning curve (as in Fig. 4).

Other authors (e.g. Nelson & Frost, 1978; Blakemore & Tobin, 1972), however, claim that since the surround suppression is broadly tuned for orientation, it should serve to sharpen the cell's orientation-tuning curve. The debate again concerns the breadth of tuning of the suppression. Results in this paper (see "Relative responses are independent of contrast") show that the normalization still works properly as long as the suppression is sufficiently broad compared to the excitatory tuning of the underlying linear operators.

There is some evidence that surround suppression is quite broadly tuned for orientation and spatial frequency. For some cells, surround suppression is not at all orientation selective, i.e. there is equal suppression from all orientations. At this time, however, it is difficult to give quantitative estimates of the tuning widths because there is no consensus in the data. Indeed, there are some puzzling contradictory results. For example, Robson et al. (1991) used a cross-orientation suppression stimulus (mask grating orthogonal to preferred orientation) to measure the size of the suppressive region, and found that it was about the same size as the classical receptive field. On the other hand, Bonds et al. (1990) found the opposite result, that suppressive surrounds were extremely large (up to 35 deg).

End-/side-stopping

Many striate cells are end-stopped and/or side-stopped, that is, they first increase then decrease their response rates as a stimulus is either lengthened or widened (Hubel & Wiesel, 1965;

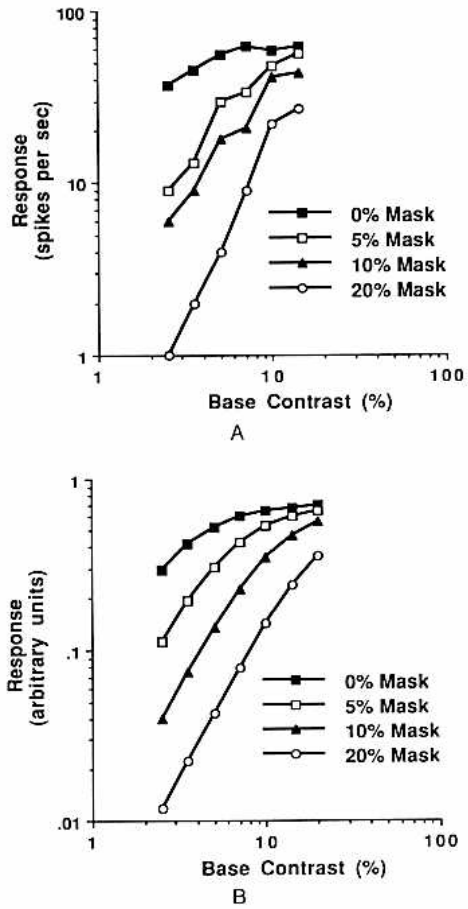

Fig. 8. A: Contrast dependence of cross-orientation suppression measured from a simple cell, replotted from Bonds (1989). Base grating was optimally oriented and mask grating oriented at the limit of the cell's orientation tuning curve. Each curve is the response for a fixed mask contrast, as the base contrast is varied. B: Contrast dependence of cross-orientation suppression for a model complex cell, with $\sigma = 0.03$. Mask grating is oriented 60 deg from optimum near the limit of the orientation-tuning curve. Lateral shift as a function of mask contrast indicates divisive suppression.

Dreher, 1972; Gilbert, 1977; Rose, 1977; Kato et al., 1978; DeValois et al., 1985; Hammond & Ahmed, 1985; Bolz & Gilbert, 1986; Murphy & Sillito, 1987; DeAngelis et al., 1990). End- and side-stopped cells were originally called hypercomplex cells by Hubel and Weisel (1965) to distinguish them from simple and complex cells, but it is now widely believed that hypercomplex cells are subtypes of the simple and complex types.

One hypothesis is that end-/side-stopping and surround suppression are mediated by the same mechanism. There is no consensus on this point. Some physiologists use the terms "end-/side-stopping" and "suppressive surround" interchangeably. Nelson and Frost (1978) and DeAngelis et al. (1990, 1992), however, argue that end-/side-stopping and nonspecific suppression are qualitatively different phenomena.

Origin of nonspecific suppression

Several authors have suggested that nonspecific suppression is intracortical and that it stems from complex cells (Bishop et al., 1973; Morrone et al., 1982; DeValois & Tootell, 1983; Bonds, 1989). Bonds (1989), for example, failed to find cross-orientation suppression in the responses of geniculate cells. He concluded that suppression must be intracortical. Morrone et al. (1982) used noise stimuli to excite cells, and then superimposed suppressive counterphase gratings. They found that for both simple and complex cells the suppression is frequency doubled; that is, it varies as the second harmonic of the stimulus temporal frequency. Morrone et al. (1982) concluded that complex cells are prime candidates as the source of the suppression, since complex cells exhibit responses to counterphase gratings that vary over time at twice the temporal frequency of the stimulus.

In the model, the suppression is intracortical but it need not come from complex cells. Model complex cell responses are sums of simple cell responses. The suppression could just as well come from a number of simple cells or from a combination of simple and complex cells.

As discussed above, extracellular recordings indicate that nonspecific suppression is divisive. Douglas et al. (1988) used intracellular recording techniques to look for evidence of divisive suppression. They found hyperpolarization of a simple cell, that corresponds to subtractive inhibition, when an optimally oriented bar was moved into an inhibitory subregion. They did not, however, find evidence for divisive suppression when the stimulus was turned 90 deg to the optimal orientation. This is at odds with the extracellular measurements of cross-orientation suppression. Douglas et al. might have missed the suppression because of difficulties with the technique, or they might have used a stimulus (a single bar instead of a grating) inadequate for revealing the suppression. In the model, the suppression arises from a feedback network that takes some amount of time to reach steady state. Thus, it would be more difficult to measure the suppression using individual bars.

Unification of suppressive mechanisms

A working hypothesis is that each cell in the striate cortex is suppressed by every other cell that is within some physical distance in the brain (see Bonds, 1989, for a similar suggestion). This predicts suppression with different characteristics for each cell, depending on the layout of orientation columns, the layout of ocular-dominance columns, the spatial inhomogeneity of the cortical map, and the layout of spatial-frequency tuning. As mentioned above, these differences are not significant, as long as suppression is broad compared to the excitatory tuning of the underlying linear operators.

Some researchers have argued that suppression is mediated by a number of independent mechanisms, e.g. that side-suppression, end-suppression, and cross-orientation suppression are independent phenomena, each resulting from a separate mechanism. At this time, however, there is no convincing evidence to disprove the unification hypothesis. It seems that the simpler unified model should be the default until there is evidence to disprove it.

Discussion

For some years, simple cells have been modeled as half-wave-rectified linear operators, and complex cells have been modeled as energy mechanisms. A variety of experimental results provide evidence in support of the linear/energy model, but many other experimental results cannot be explained by that model. To explain a larger body of physiological data, this paper suggests

modifying the linear/energy model by including divisive normalization. It is argued that divisive normalization is a critical component of cortical function since cortical cells have a limited dynamic range.

In a companion paper (Heeger, 1992*a*), a variety of additional data on striate cell responses are reviewed. Some of these data were already consistent with the linear/energy model. One of the points of that paper is to demonstrate that the new model does just as well. The main issue discussed (Heeger, 1992*a*) concerns the role of squaring in the model. Squaring is important for several reasons. First, ideal energy mechanisms require squaring to give truly phase-independent responses. Second, the underlying linear operators tile the spatiotemporal frequency domain, so that the sum of their *squared* responses gives the total Fourier energy of the stimulus. Third, given that the model complex cells outputs are squared, the model simple cell outputs must also be squared (half-squared) for the feedback normalization to work properly.

In that paper (Heeger, 1992*a*), physiological measurements of cat striate cell responses are reviewed, and the squaring hypothesis tested. Data on complex cell responses are reviewed, and it is shown that the energy model, with its underlying squaring nonlinearity, is consistent with most of the data. In addition, physiological data on simple cell responses are reviewed, comparing three models of simple cell rectification: half-wave rectification, over-rectification, and half-squaring. Some of the experimental results can be explained simply with half-wave rectification. For those cases, it is shown that half-squaring does just as well. Some of the experimental results are inconsistent with half-wave rectification, and it is shown that nearly all of those results can be explained by half-squaring.

A third paper (in preparation) presents a model of how the brain might combine inputs from the LGN to yield the linear operators that underlie model simple cell responses. The underlying linear operator of a simple cell could be achieved by a complementary arrangement of geniculate inputs (e.g. as proposed by Glezer et al., 1980, 1982). An excitatory subregion of the receptive field would result from excitation by "ON" center geniculate cells and inhibition by "OFF" center cells. Likewise, an inhibitory subregion would result from inhibition by "ON" center geniculates and excitation by "OFF" center geniculates. Each simple cell subregion would receive complementary inputs both from "ON" center and "OFF" center geniculates. Assuming that the geniculate cells are themselves (approximately) linear operators, this complementary arrangement of inputs would yield a linear operator. This complementary arrangement of geniculate inputs has been called the push-pull model.

There are a variety of experimental tests of the complementary arrangement of inputs, that characterizes the push-pull model. These experiments typically involve selectively measuring (or turning off) one set of inputs (e.g. selectively measuring inhibitory/excitatory postsynaptic potentials, using 4- amino-2-phosphonobuturic acid to suppresses activity in "ON" center retinal ganglion cells, using bicuculline to block the GABA receptors that are thought to mediate cortical inhibition). Although the experiments to date yield some conflicting results, the model is consistent with nearly all of the data.

Together, these three papers are a thorough review of cat striate physiology. The new model explains much of the existing experimental data on striate cell responses, and provides a theoretical framework in which to carry out future research on striate cortical function.

Unexplained results

Although the new model explains a large body of data, there are some experimental results with which it is not consistent. These unexplained results are listed below. Although the model does not currently explain these results, it might be refined/extended to resolve some of them.

1. Dean and Tolhurst (1986) found that simple cell response phase varies with stimulus contrast, for both counterphase gratings and temporally modulated bar stimuli.

2. There are some effects of adaptation that cannot be explained by a change of gain (see section "Contrast gain control").

3. Normalization predicts that there be only suppression from the surround. Some researchers have found enhancement (in addition to suppression) from stimulation outside of the classical receptive field (Maffei & Fiorentini, 1976; Nelson & Frost, 1978; Gilbert & Wiesel, 1990). DeAngelis et al. (1992), however, argue that the reports of surround facilitation are misleading, since they depend on how one measures the size of the excitatory receptive field. Using their procedure, DeAngelis et al. (1992) found no evidence for surround facilitation.

4. Tolhurst et al. (1980) found nonlinearities in the temporal response of striate cells. They used counterphase gratings to measure the temporal-frequency tunings of cells, and they measured responses to stationary gratings presented in long (2-s) flashes. They found that responses to the long flashes are much more transient than would be predicted by the temporal-frequency tuning curves. This is not consistent with spatiotemporal linear models. There may, however, be a way to reconcile this result with the new model. The feedback normalization in the model must be averaged over time to avoid unstable oscillations in the response (see the Appendix). The initial transient peak measured by Tolhurst et al. (1980) might be explained by this lag in feedback normalization.

5. Dean et al. (1982) measured simple cell responses for counterphase gratings and for sums of two counterphase gratings. The responses to a high temporal-frequency grating were enhanced by the addition of a low temporal frequency, and the responses to a low-frequency grating were relatively depressed in the compound stimulus. This nonlinearity in the temporal response of simple cells might be explained by divisive suppression. By analogy with Fig. 6, the response of a model cell may be either suppressed or enhanced by superimposing a second grating. For preferred temporal frequencies the response will be enhanced. For nonpreferred temporal frequencies it will be suppressed.

6. Holub and Morton-Gibson (1981) found that temporal-frequency tuning and temporal-frequency bandwidth can both vary with contrast. Once again, it might be possible to explain this result with divisive suppression. I have found, for example, that if the suppression is tuned to a relatively narrow band of temporal frequencies (e.g. the suppressive signal is pooled from a subset of cells that prefer low temporal frequencies), then the temporal-frequency tuning curves shift systematically with contrast. Note that the suppression still

acts as normalization if each and every cell is suppressed by the same temporal-frequency range.

7. There are some cells that have properties intermediate between those of standard simple and complex cells. For example, some complex cells have modulated responses to some drifting gratings (Pollen et al., 1978; Movshon et al., 1978*b*; Glezer et al., 1980; Holub & Morton-Gibson, 1981; Kulikowski et al., 1981; Kulikowski & Bishop, 1982). It is possible that these cells are actually simple cells with partially overlapping "ON" and "OFF" subregions. It is also possible that these cells are imperfectly constructed energy mechanisms. A nonlinearity other than squaring would give modulated responses (a model using absolute value instead of squaring was proposed by Pollen and Ronner, 1983). Modulated responses could also arise if the phase differences between the four input simple cells were not precisely 90 deg, or if the four operators had different spatial positions, different spatiotemporal-frequency tuning curves, or different gains (as suggested by Pollen et al., 1989).

8. Cortical physiologists have long debated whether complex cells receive inputs from simple cells or directly from the LGN. This paper follows the hypothesis, originally suggested by Hubel and Weisel (1962), that complex cells receive inputs primarily from simple cells. This is not, however, a critical aspect of the model. The energy mechanisms could also be built directly from geniculate inputs, although this would essentially require duplicating the processing that is already being done by the simple cells. There is some evidence in favor of Hubel and Weisel's hypothesis of sequential processing from geniculate to simple to complex cells. Most importantly, complex cells are uncommon in the cortical layers that are the principal destinations of LGN fibers (Hubel & Weisel, 1962; Stone & Dreher, 1973; Singer et al., 1975; Gilbert, 1977; Bullier & Henry, 1979*c*; Dean & Tolhurst, 1983). In addition, there are no systematic differences between the spatiotemporal-frequency tuning curves of simple and complex cells (Movshon et al., 1978*c*), nor between their contrast–response curves (Dean, 1981; Albrecht & Hamilton, 1982). On the other hand, there are a number of results that argue against the sequential processing of visual information from geniculate to simple to complex cells. First, Hammond and MacKay (1977) found that simple cells do not generally respond to fields of random noise whereas complex cells do. Second, complex cells respond to bars moving with faster velocities than do simple cells (Pettigrew et al., 1968; Movshon, 1975). Third, a number of studies (Hoffman & Stone, 1971; Stone & Dreher, 1973; Singer et al., 1975; Bullier & Henry, 1979*a*,*b*) have found that some complex cells can be activated by electrical stimulation from precortical visual areas with response latencies so short as to require direct connections with the LGN. Fourth, Tanaka (1983, 1985) recorded simultaneously from geniculate and striate neurons, and used cross-correlation analysis to establish connectivity between pairs of cells. He found that the delay time from the LGN to simple cells is typically the same as the delay time from the LGN to complex cells. In most cases, the delays were so short as to require direct connections between geniculate and complex cells. Fifth, Toyama et al. (1981), using a similar cross-correlation analysis, did not find excitation from simple to complex cells. Finally, intracellular recordings provide evidence for direct connections from geniculate to complex cells (Ferster & Lindstrom, 1983; Martin & Whitteridge, 1984).

9. Physiologists (Reid et al., 1987, 1991; McLean & Palmer, 1989; Emerson & Citron, 1989; Tolhurst & Dean, 1991; Albrecht & Geisler, 1991) have found that the spatiotemporal linear model does not completely account for simple cell direction selectivity. By comparing responses to counterphase gratings and drifting gratings (drifting in the preferred and anti-preferred directions), several of these researchers (Reid et al., 1987, 1991; Tolhurst & Dean, 1991; Albrecht & Geisler, 1991) demonstrated that there is a nonlinear contribution to simple cell responses. Specifically they found (1) the linear prediction from counterphase gratings underestimates a directional index computed from drifting grating responses; (2) the linear prediction correctly estimates responses to gratings drifting in the preferred direction; and (3) the linear prediction underestimates responses to gratings drifting in the anti-preferred direction, i.e. the nonlinear behavior of cells is manifested primarily as suppression of the anti-preferred response, rather than as enhancement of the preferred response. Clearly, these results refute the linear model of simple cells. Albrecht and Geisler (1991) and Heeger (1991, 1992*a*) both showed that half-squaring (or some other accelerating nonlinearity) can account for the first of these three results. However, half-squaring alone does not explain the second and third results. Some preliminary simulations with the normalized half-squared model have been conducted (Heeger, 1992*b*). Including divisive normalization contributes to the discrepancy between responses to counterphase and drifting gratings, in such a way as to suppress the anti-preferred response. These initial results, although promising, are preliminary and a number of issues need to be addressed. Tolhurst and Dean (1991) found some cells for which the linear prediction was particularly bad. It is not yet clear that these extreme cases will be accounted for by half-squaring and normalization.

Proposed experiments

A number of new experiments could be done to further test the model. Some examples follow:

1. For a particular cell, the parameters of the model can be measured and compared using different experiments. For example, the exponent, n, and threshold, T, can be measured by fitting contrast–response data to eqn. (8). These parameters might also be measured by fitting the data of Reid et al. (1987) (see Heeger 1991, for discussion).

2. The contrast–response curve of model cells shifts downward and slightly rightward if the spatial frequency of the test grating is nonoptimal (Fig. 8). The amount of rightward shift depends, in a known way, on the breadth of tuning of the suppression. For a particular cell, one should be able to predict the breadth of tuning from the shift in contrast–response (and *vice versa*).

3. The gain, σ, was varied to model both cross-orientation suppression data (Figs. 5 *vs.* 6) and contrast–response data (Fig. 2). By comparing the cross-orientation simulations in Figs. 5 and 6, it is evident that both the absolute response level and the amount of enhancement/suppression are ef-

fected by changing σ. The model predicts that changing the gain of a real cell (e.g. by brief adaptation to a higher contrast stimulus) should bring about a corresponding change in cross-orientation suppression.

4. Is surround suppression divisive? The hypothesis of this paper (see also Bonds, 1989) is that the various suppressive phenomena (e.g. surround-suppression and cross-orientation suppression) are mediated by the same underlying mechanism. If surround suppression is not divisive, then this is strong evidence against the unification hypothesis. One could answer this question by taking measurements analogous to those in Fig. 8. A base grating (of preferred spatiotemporal frequency) would be presented to a cell's receptive-field center. A second (mask) grating would be presented in the surround. One would measure a series of contrast-response curves, each with a different mask contrast. If surround suppression is divisive, increasing the mask contrast will lead to a lateral shift (on a log-contrast axis) of the contrast-response curves.

5. There is a straightforward experiment that tests directly for the underlying linearity of simple cells, independent of the rectification and independent of divisive suppression. Consider stimuli made up of two spots (or bars) at fixed positions that are both modulated sinusoidally over time. Both spots have the same temporal frequency, but the amplitude and phase of modulation may be different. For a spatiotemporal linear operator, one can always choose the relative amplitude and phase of modulation, regardless of the positions of the two spots, to null the output. This is also true for a normalized, rectified linear operator. An experiment of this sort was performed by Spekreijse and van den Berg (1971) in goldfish retinal ganglion cells. It is surprising that this experiment has not yet been done in the cortex. Tolhurst and Dean (1987) performed experiments on cat cortical cells using pairs of temporally modulated bars, but they did not try to null the responses [see Heeger (1992*a*) for summary and explanation of their data in the context of the half-squaring normalization model].

Summary

The new model, with divisive normalization, explains a number of physiological results that cannot be explained by the linear/energy model:

1. Model cell responses saturate at high contrasts. The contrast-response curves of model cells are very similar to those of real cells (Fig. 2).
2. The gain of model cells can be adjusted, resulting in adaptation (Fig. 2).
3. Model cells exhibit nonspecific suppression (Figs. 5–7).
4. Nonspecific suppression is divisive (Fig. 8).
5. Contrast-response curves of model cells shift mostly downward for nonoptimal stimuli (Fig. 3), and the tuning widths of model cells are largely independent of contrast (Fig. 4). In other words, the ratio of responses produced by two different stimuli is largely invariant with respect to stimulus contrast. In this way, information about a visual stimulus, other than its contrast, is represented as the relative responses of a collection of cells.
6. The contrast-response functions for visual neurons are well modeled by the hyperbolic ratio function (see section "Contrast-response"). In the model, contrast-response functions are hyperbolic ratios with exponents of 2. Physiologists have found that the exponent in the contrast-response functions is 2 on average, but there is variability from cell to cell. Varying the threshold and gain [T and σ in eqn. (8)] simultaneously can look very much like a change in the exponent [n in eqn. (8)]. This suggests the possibility of fitting contrast-response data with a fixed exponent, accounting for the variability from cell to cell by changing the values of T and σ.

Physiologists have long debated the role of intracortical (e.g. cross-orientation) suppression. Some researchers have argued that broadly tuned suppression sharpens a cell's tuning properties. Others have proposed that selectivity of cortical cells results from suppressive interactions.

According to the model advocated in this paper, a cell is selective for orientation, scale, and direction of motion because of the underlying spatiotemporal linear operators. Divisive suppression does not contribute to selectivity in the model. Rather, it acts to normalize cell responses. The ratio of the normalized responses of two model cells equals the ratio of their underlying unnormalized responses. Divisive suppression merely acts to rescale both by the *same* factor.

Perfect normalization would require that all cells be suppressed by exactly the same factor. The results in Fig. 3 show that broadly tuned suppression behaves only slightly differently. The normalization works properly as long as the suppression is sufficiently broad compared to the excitatory tuning of the underlying linear operators. How broad must the suppression be? In the present implementation of the model, the excitatory spatial-frequency bandwidth is about one octave and the normalization is summed over three spatial-frequency bands. This 3:1 ratio in tuning widths is certainly sufficient (see Figs. 3 and 4).

For some cells it may be the case that suppression has a significant effect on tuning, but for most cells it appears that suppression is broad enough that it has little or no impact on tuning.

Acknowledgments

This research was supported by the MIT Media Laboratory, by NASA-Ames Grant NCC2-307, and by NASA RTOP 506-71-51. This paper benefited greatly from discussions with Ted Adelson, Beau Watson, Jim Bergen, John Robson, A. B. Bonds, Tony Movshon, Brian Wandell, E. J. Chichilnisky, and Lee Stone.

References

Adelson, E.H. & Bergen, J.R. (1985). Spatiotemporal energy models for the perception of motion. *Journal of the Optical Society of America A* **2**, 284–299.

Albrecht, D.G., Farrar, S.B. & Hamilton, D.B. (1984). Spatial contrast adaptation characteristics of neurones recorded in the cat's visual cortex. *Journal of Physiology* (London) **347**, 713–739.

Albrecht, D.G. & Geisler, W.S. (1991). Motion sensitivity and the contrast-response function of simple cells in the visual cortex. *Visual Neuroscience* **7**, 531–546.

Albrecht, D.G. & Hamilton, D.B. (1982). Striate cortex of monkey

and cat: Contrast response function. *Journal of Neurophysiology* **48**, 217–237.

BISHOP, P.O., COOMBS, J.S. & HENRY, G.H. (1973). Receptive fields of simple cells in the cat striate cortex. *Journal of Physiology* (London) **231**, 31–60.

BLAKEMORE, C. & TOBIN, E.A. (1972). Lateral inhibition between orientation detectors in the cat's visual cortex. *Experimental Brain Research* **15**, 439–440.

BOLZ, J. & GILBERT, C.D. (1986). Generation of end-inhibition in the visual cortex *via* interlaminar connections. *Nature* **320**, 362–365.

BONDS, A.B. (1989). Role of inhibition in the specification of orientation selectivity of cells in the cat striate cortex. *Visual Neuroscience* **2**, 41–55.

BONDS, A.B. (1991). Temporal dynamics of contrast gain in single cells of the cat striate cortex. *Visual Neuroscience* **6**, 239–255.

BONDS, A.B., DEBUSK, B.C. & MING, S. (1990). Stimulation far beyond the receptive field of cat striate cortical cells strongly mediates responsiveness: A mechanism for global inhibition. *Investigative Opthalmology and Visual Science* (Suppl.) **31**, 429.

BULLIER, J. & HENRY, G.H. (1979*a*). Ordinal position of neurons in cat striate cortex. *Journal of Neurophysiology* **42**, 1251–1263.

BULLIER, J. & HENRY, G.H. (1979*b*). Neural path taken by afferent streams in striate cortex of the cat. *Journal of Neurophysiology* **42**, 1264–1270.

BULLIER, J. & HENRY, G.H. (1979*c*). Laminar distribution of first-order neurons and afferent terminals in cat striate cortex. *Journal of Neurophysiology* **42**, 1271–1281.

CAMPBELL, F.W., COOPER, G.F. & ENROTH-CUGELL, C. (1968). The angular selectivity of visual cortical cells to moving gratings. *Journal of Physiology* (London) **198**, 237–250.

CAMPBELL, F.W., COOPER, G.F. & ENROTH-CUGELL, C. (1969). The spatial selectivity of visual cells of the cat. *Journal of Physiology* (London) **203**, 223–235.

CHAO-YI, LI. & CREUTZFELDT, O. (1984). The representation of contrast and other stimulus parameters by single neurons in area 17 of the cat. *Pflugers Archives* **401**, 304–314.

DEAN, A.F. (1980). The contrast-dependence of direction selectivity. *Journal of Physiology* (London) **303**, 38p–39p.

DEAN, A.F. (1981). The relationship between response amplitude and contrast for cat striate cortical neurones. *Journal of Physiology* (London) **318**, 413–427.

DEAN, A.F. (1983). Adaptation-induced alteration of the relation between response amplitude and contrast in cat striate cortical mechanisms. *Vision Research* **23**, 249–256.

DEAN, A.F., HESS, R.F. & TOLHURST, D.J. (1980). Divisive inhibition involved in direction selectivity. *Journal of Physiology* (London) **308**, 84p–85p.

DEAN, A.F. & TOLHURST, D.J. (1983). On the distinctiveness of simple and complex cells in the visual cortex of the cat. *Journal of Physiology* (London) **344**, 305–325.

DEAN, A.F. & TOLHURST, D.J. (1986). Factors influencing the temporal phase of response to bar and grating stimuli for simple cells in the cat striate cortex. *Experimental Brain Research* **62**, 143–151.

DEAN, A.F., TOLHURST, D.J. & WALKER, N.S. (1982). Nonlinear temporal summation by simple cells in cat striate cortex demonstrated by failure of superposition. *Experimental Brain Research* **45**, 456–458.

DEANGELIS, G.C., OHZAWA, I., FREEMAN, R.D. & GHOSE, G. (1990). Properties of length and width tuning of cells in the cat's striate cortex. *Investigative Opthalmology and Visual Science* (Suppl.) **32**, 430.

DEANGELIS, G.C., ROBSON, J.G., OHZAWA, I. & FREEMAN, R.D. (1992). The organization of suppression in receptive fields of neurons in the cat's visual cortex. *Journal of Neurophysiology* (in press).

DEBRUYN, E.J. & BONDS, A.B. (1986). Contrast adaptation in the cat is not mediated by GABA. *Brain Research* **383**, 339–342.

DERRINGTON, A.M. & LENNIE, P. (1984). Spatial and temporal contrast sensitivities of neurones in lateral geniculate nucleus of macaque. *Journal of Physiology* (London) **357**, 219–240.

DEVALOIS, K. & TOOTELL, R. (1983). Spatial-frequency-specific inhibition in cat striate cortex cells. *Journal of Physiology* (London) **336**, 359–376.

DEVALOIS, R.L., THORELL, L.G. & ALBRECHT, D.G. (1985). Periodicity of striate-cortex-cell receptive fields. *Journal of the Optical Society of America A* **2**, 1115–1123.

DOUGLAS, R.J., MARTIN, K.A.C. & WHITTERIDGE, D. (1988). Selective responses of visual cortical cells do not depend on shunting inhibition. *Nature* **332**, 642–644.

DREHER, B. (1972). Hypercomplex cells in the cat's striate cortex. *Investigative Opthalmology* **11**, 355–356.

EMERSON, R.C. & CITRON, M.C. (1989). Linear and nonlinear mechanisms of motion selectivity in single neurons of the cat's visual cortex. In *Proceedings of IEEE International Conference on Systems, Man, and Cybernetics*, ed. pp. 448–453. Cambridge, Massachusetts: IEEE.

FERSTER, D. (1981). A comparison of binocular depth mechanisms in areas 17 and 18 of the cat visual cortex. *Journal of Physiology* (London) **311**, 623–655.

FERSTER, D. & LINDSTROM, S. (1983). An intracellular analysis of geniculo-cortical connectivity in area 17 of the cat. *Journal of Physiology* (London) **342**, 181–215.

FREEMAN, R.D., OHZAWA, I. & ROBSON, J.G. (1987). A comparison of monocular and binocular inhibitory processes in the visual cortex of cat. *Journal of Physiology* (London) **396**, 69p.

GILBERT, C.D. (1977). Laminar differences in receptive properties of cells in cat primary visual cortex. *Journal of Physiology* (London) **268**, 391–421.

GILBERT, C.D. & WIESEL, T.N. (1990). The influence of contextual stimuli on the orientation selectivity of cells in primary visual cortex of the cat. *Vision Research* **30**, 1689–1701.

GLEZER, V.D., TSCHERBACH, T.A., GAUSELMAN, V.E. & BONDARKO, V.E. (1980). Linear and nonlinear properties of simple and complex receptive fields in area 17 of the cat visual cortex. *Biological Cybernetics* **37**, 195–208.

GLEZER, V.D., TSCHERBACH, T.A., GAUSELMAN, V.E. & BONDARKO, V.E. (1982). Spatio-temporal organization of receptive fields of the cat striate cortex. *Biological Cybernetics* **43**, 35–49.

GULYAS, B., ORBAN, G.A., DUYSENS, J. & MAES, H. (1987). The suppressive influence of moving textured backgrounds on responses of cat striate neurons to moving bars. *Journal of Neurophysiology* **57**, 1767–1791.

HAMMOND, P. & AHMED, B. (1985). Length summation of complex cells in cat striate cortex: A reappraisal of the special/standard classification. *Neuroscience* **15**, 639–649.

HAMMOND, P. & MACKAY, D.M. (1977). Differential responsiveness of simple and complex cells in cat striate cortex to visual texture. *Experimental Brain Research* **30**, 275–296.

HAMMOND, P. & MACKAY, D.M. (1978). Modulation of simple cell activity in cat by moving textured backgrounds. *Journal of Physiology* (London) **284**, 117p.

HAMMOND, P. & MACKAY, D.M. (1981). Modulatory influences of moving textured backgrounds on responsiveness of simple cells in feline striate cortex. *Journal of Physiology* (London) **319**, 431–442.

HAMMOND, P., MOUAT, G.S. & SMITH, A.T. (1985). Motion after-effects in cat striate cortex elicited by moving gratings. *Experimental Brain Research* **60**, 411–416.

HAMMOND, P., MOUAT, G.S. & SMITH, A.T. (1986). Motion after-effects in cat striate cortex elicited by moving texture. *Vision Research* **26**, 1055–1060.

HAMMOND, P., MOUAT, G.S. & SMITH, A.T. (1988). Neural correlates of motion after-effects in cat striate cortical neurones: Monocular adaptation. *Experimental Brain Research* **72**, 1–20.

HAMMOND, P., POMFRETT, C.J.D. & AHMED, B. (1989). Neural motion after-effects in the cat's striate cortex: Orientation selectivity. *Vision Research* **29**, 1671–1683.

HATA, Y., TSUMOTO, T., SATO, H., HAGIHARA, K. & TAMURA, H. (1988). Inhibition contributes to orientation selectivity in visual cortex of cat. *Nature* **335**, 815–817.

HEEGER, D.J. (1990). Nonlinear model of cat striate physiology. *Society for Neuroscience Abstracts* **16**, 229.

HEEGER, D.J. (1991). Nonlinear model of neural responses in cat visual cortex. In *Computational Models of Visual Processing*, ed. LANDY, M., MOVSHON, J.A., pp. 119–133. Cambridge, Massachusetts: MIT Press.

HEEGER, D.J. (1992*a*). Half-squaring in responses of cat simple cells. *Visual Neuroscience* (in press).

HEEGER, D.J. (1992*b*). Modeling simple cell direction selectivity with normalized, half-squared, linear operators. *Investigative Ophthalmology and Visual Science* (Suppl.) **33** (in press).

HEEGER, D.J. & ADELSON, E.H. (1989). Nonlinear model of cat striate cortex. *Optics News* **15**, A-42.

HESS, R., NEGISHI, K. & CREUTZFELDT, O.D. (1975). The horizontal spread of intracortical inhibition in the visual cortex. *Experimental Brain Research* **22**, 415–419.

HOFFMAN, K.P. & STONE, J. (1971). Conduction velocity of afferent to cat visual cortex: A correlation with cortical receptive fields of single cells in cat striate cortex. *Brain Research* **32**, 460–466.

HOLUB, R.A. & MORTON-GIBSON, M. (1981). Response of visual cortical neurons of the cat to moving sinusoidal gratings: Response-contrast functions and spatiotemporal integration. *Journal of Neurophysiology* **46**, 1244–1259.

HUBEL, D. & WIESEL, T. (1962). Receptive fields, binocular interaction, and functional architecture in the cat's visual cortex. *Journal of Physiology* (London) **160**, 106–154.

HUBEL, D. & WIESEL, T. (1965). Receptive field and functional architecture in two nonstriate visual areas (18–19) of the cat. *Journal of Neurophysiology* **28**, 229–289.

KAJI, S. & KAWABATA, N. (1985). Neural interactions of two moving patterns in the direction and orientation domain in the complex cells of cat's visual cortex. *Vision Research* **25**, 749–753.

KATO, H., BISHOP, P.O. & ORBAN, G.A. (1978). Hypercomplex and simple/complex cell classifications in cat striate cortex. *Journal of Neurophysiology* **41**, 1071–1095.

KULIKOWSKI, J.J. & BISHOP, P.O. (1982). Silent periodic cells in the cat striate cortex. *Vision Research* **22**, 191–200.

KULIKOWSKI, J.J., BISHOP, P.O. & KATO, H. (1981). Spatial arrangement of responses by cells in the cat visual cortex to light and dark bars and edges. *Experimental Brain Research* **44**, 371–385.

MADDESS, T., MCCOURT, M.E., BLAKESLEE, B. & CUNNINGHAM, R.B. (1988). Factors governing the adaptation of cells in area 17 of the cat visual cortex. *Biological Cybernetics* **59**, 229–236.

MAFFEI, L. & FIORENTINI, A. (1973). The visual cortex as a spatial-frequency analyzer. *Vision Research* **13**, 1255–1267.

MAFFEI, L. & FIORENTINI, A. (1976). The unresponsive regions of visual cortical receptive fields. *Vision Research* **16**, 1131–1139.

MAFFEI, L., FIORENTINI, A. & BISTI, S. (1973). Neural correlate of perceptual adaptation to gratings. *Science* **182**, 1036–1038.

MARLIN, S.G., HASAN, S.J. & CYNADER, M.S. (1988). Direction-selective adaptation in simple and complex cells in cat striate cortex. *Journal of Neurophysiology* **59**, 1314–1330.

MARTIN, K.A.C. & WHITTERIDGE, D. (1984). Form, function and intracortical projections of spiny neurones in the striate visual cortex of the cat. *Journal of Physiology* (London) **353**, 463–504.

MCLEAN, J. & PALMER, L.A. (1989). Contribution of linear spatiotemporal receptive-field structure to velocity selectivity of simple cells in area 17 of cat. *Vision Research* **29**, 675–679.

MORRONE, M.C., BURR, D.C. & MAFFEI, L. (1982). Functional implications of cross-orientation inhibition of cortical visual cells. *Proceedings of the Royal Society B* (London) **216**, 335–354.

MOVSHON, J.A. (1975). The velocity tuning of single units in cat striate cortex. *Journal of Physiology* (London) **249**, 445–468.

MOVSHON, J.A. & LENNIE, P. (1979). Pattern-selective adaptation in visual cortical neurones. *Nature* **278**, 850–852.

MOVSHON, J.A., THOMPSON, I.D. & TOLHURST, D.J. (1978*a*). Spatial summation in the receptive fields of simple cells in the cat's striate cortex. *Journal of Physiology* (London) **283**, 53–77.

MOVSHON, J.A., THOMPSON, I.D. & TOLHURST, D.J. (1978*b*). Receptive-field organization of complex cells in the cat's striate cortex. *Journal of Physiology* (London) **283**, 79–99.

MOVSHON, J.A., THOMPSON, I.D. & TOLHURST, D.J. (1978*c*). Spatial and temporal contrast sensitivity of neurones in areas 17 and 18 of the cat's visual cortex. *Journal of Physiology* (London) **283**, 101–120.

MURPHY, P.C. & SILLITO, A.M. (1987). Corticofugal feedback influences the generation of length tuning in the visual pathway. *Nature* **329**, 727–729.

NELSON, J.I., LINGNER, I. & BREMMER, F. (1991). Adaptation and disadaptation in cat A17 cells stimulated only beyond their classic receptive fields. *Investigative Ophthalmology and Visual Science* (Suppl.) **32**, 1252.

NELSON, J.J. & FROST, B.J. (1978). Orientation-selective inhibition from beyond the classic visual receptive field. *Brain Research* **139**, 359–365.

NELSON, S.B. (1991). Temporal interactions in the cat visual system. I. Orientation-selective suppression in visual cortex. *Journal of Neuroscience* **11**, 344–356.

OHZAWA, I. & FREEMAN, R.D. (1986). The binocular organization of simple cells in the cat's visual cortex. *Journal of Neurophysiology* **56**, 221–242.

OHZAWA, I., SCLAR, G. & FREEMAN, R.D. (1982). Contrast gain control in the cat visual cortex. *Nature* **298**, 266–268.

OHZAWA, I., SCLAR, G. & FREEMAN, R.D. (1985). Contrast gain control in the cat's visual system. *Journal of Neurophysiology* **54**, 651–667.

PETTIGREW, J.D., NIKARA, T. & BISHOP, P.O. (1968). Responses to moving slits by single units in cat striate cortex. *Experimental Brain Research* **6**, 373–390.

POLLEN, D. & RONNER, S. (1983). Visual cortical neurons as localized spatial-frequency filters. *IEEE Transactions on Systems, Man, and Cybernetics* **13**, 907–916.

POLLEN, D.A., ANDREWS, B.W. & FELDON, S.E. (1978). Spatial-frequency selectivity of periodic complex cells in the visual cortex of the cat. *Vision Research* **18**, 665–682.

POLLEN, D.A., GASKA, J.P. & JACOBSON, L.D. (1989). Physiological constraints on models of visual cortical function. In *Models of Brain Function*, ed. COTTERILL, R.M.J., Cambridge University Press.

REID, R.C., SOODAK, R.E. & SHAPLEY, R.M. (1987). Linear mechanisms of directional selectivity in simple cells of cat striate cortex. *Proceedings of the National Academy of Sciences of the U.S.A.* **84**, 8740–8744.

REID, R.C., SOODAK, R.E. & SHAPLEY, R.M. (1991). Directional selectivity and spatiotemporal structure of receptive fields of simple cells in cat striate cortex. *Journal of Neurophysiology* **66**, 505–529.

ROBSON, J.G. (1988). Linear and nonlinear operations in the visual system. *Investigative Ophthalmology and Visual Science* (Suppl.) **29**, 117.

ROBSON, J.G., DEANGELIS, G.C., OHZAWA, I. & FREEMAN, R.D. (1991). Cross-orientation inhibition in cat cortical cells originates from within the receptive field. *Investigative Ophthalmology and Visual Science* (Suppl.) **32**, 429.

ROSE, D. (1977). Responses of single units in cat visual cortex to moving bars of light as a function of bar length. *Journal of Physiology* (London) **271**, 1–23.

SAUL, A.B. & CYNADER, M.S. (1989*a*). Adaptation in single units in the visual cortex: The tuning of aftereffects in the spatial domain. *Visual Neuroscience* **2**, 593–607.

SAUL, A.B. & CYNADER, M.S. (1989*b*). Adaptation in single units in the visual cortex: The tuning of aftereffects in the temporal domain. *Visual Neuroscience* **2**, 609–620.

SCLAR, G. & FREEMAN, R.D. (1982). Orientation selectivity of the cat's striate cortex is invariant with stimulus contrast. *Experimental Brain Research* **46**, 457–461.

SCLAR, G., MAUNSELL, J.H.R. & LENNIE, P. (1990). Coding of image contrast in central visual pathways of the macaque monkey. *Vision Research* **30**, 1–10.

SHAPLEY, R. & ENROTH-CUGELL, C. (1984). Visual adaptation and retinal gain control. *Progress in Retinal Research* **3**, 263–346.

SINGER, W., TRETTER, F. & CYNADER, M. (1975). Organization of cat striate cortex: A correlation of receptive-field properties with afferent and efferent connections. *Journal of Neurophysiology* **38**, 1080–1098.

SKOTTUN, B.C., BRADLEY, A., SCLAR, G., OHZAWA, I. & FREEMAN, R.D. (1987). The effects of contrast on visual orientation and spatial-frequency discrimination: A comparison of single cells and behavior. *Journal of Neurophysiology* **57**, 773–786.

SPEKREIJSE, H. & VAN DEN BERG, T.J.T.P. (1971). Interaction between colour and spatial coded processes converging to retinal ganglion cells in goldfish. *Journal of Physiology* (London) **215**, 679–692.

SPERLING, G. & SONDHI, M.M. (1968). Model for visual luminance discrimination and flicker detection. *Journal of the Optical Society of America* **58**, 1133–1145.

STONE, J. & DREHER, B. (1973). Projection of X- and Y-cells of the cat's lateral geniculate nucleus to areas 17 and 18 of visual cortex. *Journal of Neurophysiology* **36**, 551–567.

TANAKA, K. (1983). Cross-correlation analysis of geniculostriate neuronal relationships in cats. *Journal of Neurophysiology* **49**, 1303–1318.

TANAKA, K. (1985). Organization of geniculate inputs to visual cortical cells in the cat. *Vision Research* **25**, 357–364.

TOLHURST, D.J. & DEAN, A.F. (1987). Spatial summation by simple cells in the striate cortex of the cat. *Experimental Brain Research* **66**, 607–620.

TOLHURST, D.J. & DEAN, A.F. (1991). Evaluation of a linear model of directional selectivity in simple cells of the cat's striate cortex. *Visual Neuroscience* **6**, 421–428.

TOLHURST, D.J., WALKER, N.S., THOMPSON, I.D. & DEAN, A.F. (1980). Nonlinearities of temporal summation in neurones in area 17 of the cat. *Experimental Brain Research* **38**, 431–435.

TOYAMA, K., KIMURA, M. & TANAKA, T. (1981). Organization of cat visual cortex as investigated by cross-correlation technique. *Journal of Neurophysiology* **46**, 202–214.

ULLMAN, S. & SCHECHTMAN, G. (1982). Adaptation and gain normalization. *Proceedings of the Royal Society B* (London) **216**, 299–313.

VAUTIN, R.G. & BERKELEY, M.A. (1977). Responses of single cells in cat visual cortex to prolonged stimulus movement: Neural correlates of visual aftereffect. *Journal of Neurophysiology* **40**, 1051–1065.

VIDYASAGAR, T.R. (1990). Pattern adaptation in cat visual cortex is a cooperative phenomenon. *Neuroscience* **36**, 175–179.

VON DER HEYDT, R., HANNY, P. & ADORJANI, C. (1978). Movement aftereffects in the visual system. *Archives of Italian Biology* **116**, 248–254.

Appendix: Feedback normalization

A simple example demonstrates how normalization can be implemented as a feedback network. A (one-input and one-output) feedback network is illustrated in Fig. 9. In this network, the single input is labeled $I(t)$ and the output is labeled $R(t)$, both of which vary over time. There are two additional parameters, σ and $R_{\max}$, that are assumed to be fixed.

The circle labeled "LP" in Fig. 9 is a spatiotemporal low-pass filter on the feedback signal, the purpose of which is to damp the feedback signal to avoid instability in the output. The output of the low-pass filter is a weighted sum of the past and present responses:

$$B(t) = \alpha R(t) + (1 - \alpha)B(t - \delta), \tag{A1}$$

where $B(t)$ is the time-averaged feedback signal, $\alpha < 1$ is a constant, and δ is a time delay. This low-pass filter has an exponentially decaying impulse response.

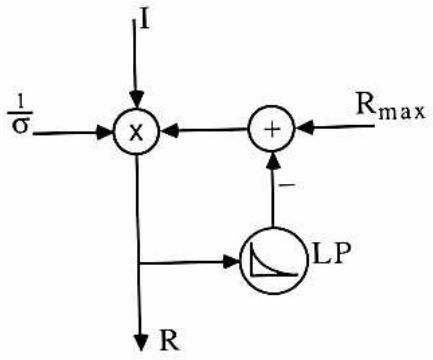

Fig. 9. Diagram of a feedback normalization network. The input is multiplied by the feedback signal, but results in divisive normalization. See text for details.

The output of the feedback network, as a function of time, is given by

$$R(t + \delta) = \frac{I(t)}{\sigma}\,[R_{\max} - B(t)]. \tag{A2}$$

In the steady state [i.e. when $I(t)$ is constant over time and when $B(t) = R(t)$], this equation can be rewritten with no dependence on time. Then, solving for R gives

$$R = R_{\max}\frac{I}{\sigma + I}, \tag{A3}$$

that has the same form as eqn. (4). It is straightforward to expand this network to have an arbitrary number of inputs and outputs, mutually feeding back on (and suppressing) one another.

This is but one example of how a feedback network can implement normalization. There are certainly other networks that achieve approximately the same result in ways that may be more biologically plausible.